

Cite this: *RSC Adv.*, 2018, 8, 20829

## Antibacterial coordination polymer hydrogels composed of silver(i)-PEGylated bisimidazolylbenzyl alcohol†

Fang Wu,<sup>a</sup> Dengfeng He,<sup>a</sup> Lei Chen,<sup>b</sup> Fangqin Liu,<sup>a</sup> Haolong Huang,<sup>a</sup> Jiangshan Dai,<sup>c</sup> Shiyong Zhang <sup>\*a</sup> and Jingsong You <sup>a</sup>

Herein, antibacterial coordination polymer hydrogels were conveniently fabricated in water *via* coordination between silver nitrate and PEGylated bisimidazolylbenzyl alcohol (**1a–c**). These coordination polymer hydrogels exhibit much better antibacterial activity than silver nitrate against both Gram-negative and Gram-positive pathogens including multidrug-resistant pathogens. The coordination polymer **Ag/1c** with a long PEG chain (PEG1000) was demonstrated to be the most effective antibacterial material, and its minimum inhibition concentrations (MICs) could be as low as 15.2 times for common *Staphylococcus aureus* and 4.8 times for methicillin-resistant *Staphylococcus aureus* over that of silver nitrate. With improved antibacterial performance, easy preparation method, improved stability, sustained releasability, outstanding ductility and low cytotoxicity, the as-prepared coordination polymer hydrogels should find various potential applications such as in clinical burn and wound dressings, biofilms, bioadhesives, and coatings of biomedical materials.

Received 23rd January 2018

Accepted 22nd May 2018

DOI: 10.1039/c8ra00682b

rsc.li/rsc-advances

## Introduction

Elemental silver has been used for centuries as an antimicrobial agent because of its broad-spectrum antimicrobial activity, low drug resistance and easy accessibility. However, silver ions are not stable and easily decompose in light; moreover, they have problem of sudden release and are sometimes toxic to normal organisms in human-related applications;<sup>1–4</sup> recently, incorporation of silver ions or silver nanoparticles into synthetic materials for the treatment of bacterial infections and/or prophylactic purpose (*e.g.*, surface treatments of water purification systems, surgical equipment, and burn and wound dressings) has attracted significant interest.<sup>5–11</sup> After incorporation, silver ions are protected in the matrix, which can easily overcome the abovementioned defects and achieve improved therapeutic effects. For example, it has been reported that long-term releasability of silver ions in the area of the superficial wound is important for accelerating the process of healing and preventing infection.<sup>12</sup>

Among various synthetic materials, the nano-sized polymer fiber can provide high surface area to contact bacteria and represents an optimal matrix for silver entrapment.<sup>13,14</sup>

Electrospinning is presently a widely used technique for the construction of polymer nano-fibers.<sup>15–20</sup> However, this method requires complicated procedures such as use of a supplementary electric potential to produce a jet as the origin of nano-fiber formation. Moreover, biodegradability of the polymers used to create nano-fibers would sometimes be an issue, which severely hinders their use in biology-related systems. Therefore, it is desirable to develop alternative nano-fibers with polymer fiber-like characteristics but with much easier preparation method and high biocompatibility.

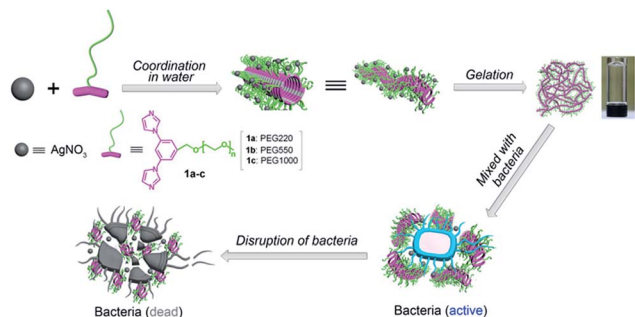
As a new class of hybrid inorganic–organic materials created by infinitely extending the metal–ligand coordination interactions, coordination polymers own a similar long chain structure as common polymers.<sup>21–24</sup> Moreover, due to the non-covalent connection mode, coordination polymers avoid complex chemical synthesis and the concern of biodegradability and thus would be expected to exhibit better performance in the construction of antibacterial nano-fibers when compared with traditional covalent polymers. To our surprise, although some metal complexes have been reported as antibacterial agents,<sup>25–31</sup> no studies have been reported regarding the utilization of coordination polymers in the fabrication of antibacterial nano-fibers.

We have previously reported a novel class of coordination polymer organogels originating from the coordination between Ag(I) and 1,3-bisimidazolyl benzene that constitutes the structurally simplest coordination polymer gels in terms of the secondary building units (SBUs), *i.e.* the minimum repeating unit for the construction of coordination polymers, reported to

<sup>a</sup>National Engineering Research Center for Biomaterials, Sichuan University, China<sup>b</sup>State Key Laboratory of Oral Diseases, West China Hospital of Stomatology, Sichuan University, China<sup>c</sup>College of Life Science, Sichuan University, China

† Electronic supplementary information (ESI) available. See DOI: 10.1039/c8ra00682b





**Scheme 1** Schematic of the fabrication of coordination polymer hydrogels for enhanced antibacterial activity.

date.<sup>32</sup> In the present study, we developed a new kind of antibacterial coordination polymer hydrogels *via* coordination between silver nitrate and PEGylated bisimidazolylbenzyl alcohol (**1a–c**) (Scheme 1). These fibrous coordination polymer hydrogels feature low critical gel concentration, outstanding ductility, excellent stability, and strong mechanical strength, reduce the cytotoxicity and improve the long-term releasability of Ag ions; moreover, they demonstrate superior antibacterial activity to silver ions in all tested bacteria, including Gram-negative, Gram-positive, and multidrug-resistant pathogens, and are believed to be highly useful as an antibacterial material for medical applications.

## Experimental

### Reagents

Unless otherwise stated, all reagents were obtained from commercial suppliers and used without further purification. Poly(ethylene glycol) monomethyl ethers ( $M_n = 200, 550$ , or  $1000 \text{ g mol}^{-1}$ ) were purchased from Sigma-Aldrich corporation. 3,5-Dibromobenzyl alcohol was purchased from Alfa Aesar. *N,N*-Dimethylglycine was purchased from ASTACH. Tosyl chloride, pyridine,  $\text{K}_2\text{CO}_3$ , NaCl and NaH were purchased from Kelong chemical reagent factory in Chengdu. Tryptone and yeast extract were purchased from OXOID. Agar was purchased from Biotopped. Trypticase Soy Broth (TSB) was purchased from Qingdao Hope Bio-Technology. Dulbecco's modified Eagle's medium and fetal bovine serum were purchased from Basal Media. MTT (3-(4,5-dimethylthiazol-2-yl)-2,5-diphenyltetrazolium bromide) was purchased from Aladdin. All solvents used for the reactions were freshly distilled prior to use. Deionized water was used in all aqueous experiments. Syntheses of the compounds **1a–c** are reported in the ESI.†

### Characterizations

Routine NMR spectra were obtained using Bruker AV II-400. The  $^1\text{H}$  NMR chemical shifts were measured relative to  $\text{CDCl}_3$  as the internal reference ( $\text{CDCl}_3$ :  $\delta$  7.26 ppm). The  $^{13}\text{C}$  NMR chemical shifts are reported using  $\text{CDCl}_3$  as the internal standard ( $\text{CDCl}_3$ :  $\delta$  76.80–77.16 ppm). Mass spectrometry was performed using a Waters Q-ToF premier instrument. The JSM-5900LV scanning

electron microscope (SEM) was used for obtaining the images at 20 kV. The preparation of samples for SEM was as follows: the hydrogel in  $\text{H}_2\text{O}$  was frozen by liquid nitrogen, and the frozen specimen was then evaporated by a vacuum pump at  $-50^\circ\text{C}$  for 1 day. The obtained xerogel was shielded with gold and then examined. Transmission electron microscopy (TEM) studies were conducted at 120 kV using a Tecnai G2F20S-TWIN instrument. The TEM specimens were prepared by gently placing a copper grid on the surface of the sample. The TEM grid was then removed, stained with phosphotungstic acid, dried for 0.5 h at room temperature, and then subjected to TEM observation. Gram-positive (*Staphylococcus aureus*, ATCC29213), methicillin-resistant (*Staphylococcus aureus*, ATCC33591), Gram-negative (*Escherichia coli*, ATCC35218) and amoxicillin-resistant (*Escherichia coli*, ATCC51299) pathogens were used to study the antibacterial activities of silver ion-decorated hydrogels. The bacteria were grown in the Luria-Bertani (LB) culture medium, containing tryptone  $10 \text{ g L}^{-1}$ , yeast extract  $5 \text{ g L}^{-1}$ , and NaCl  $10 \text{ g L}^{-1}$ , or LB solid medium in an incubator at  $37^\circ\text{C}$ . Human embryonic kidney cells (293T) were obtained from the Chinese Academy of Science Cell Bank for Type Culture Collection (Shanghai, China) and used for all the cell experiments. The cell line was grown in Dulbecco's modified Eagle's medium (DMEM) supplemented with 10% (v/v) fetal bovine serum (FBS) and 1% (v/v) penicillin/streptomycin in an incubator under 5%  $\text{CO}_2$  at  $37^\circ\text{C}$ . Cell toxicity was evaluated by measuring the percentage of cell viability *via* the MTT (3-(4,5-dimethylthiazol-2-yl)-2,5-diphenyltetrazolium bromide) assay. The absorbance at 490.0 nm was then measured using a microplate reader Varioscan Flash (ThermoFisher SCIEN-TIFIC). The cell viability (%) was obtained according to the manufacturer's instructions.

### Typical preparation of the antibacterial coordination polymer hydrogels

An aqueous (0.5 mL) solution of **1a** (8.8 mg, 0.0021 mmol) was added to an aqueous (0.5 mL) solution of  $\text{AgNO}_3$  (5.2 mg, 0.0032 mmol) in a vial under continuous shaking at room temperature in the absence of light. After the mixture was placed in the vial for about 5 min, the transparent hydrogel, which was evaluated by the “stable to inversion of a vial” method, was formed. The hydrogel obtained from this method usually has some air bubbles, which could be removed by sonication.

### Rheological measurements

The dynamic rheological measurements were performed by an advanced rheometric extended system (ARES, TA Co.) fitted with a Couette geometry (50 mm diameter) and a circulating environmental system for the control of temperature. For investigating the viscoelastic properties of the hydrogel sample **Ag/1a–c**, the values of storage modulus ( $G'$ ) and loss modulus ( $G''$ ) were measured. The angular frequency ( $\omega$ ) applied to the hydrogel sample increased from 0.1 to  $100 \text{ rad s}^{-1}$ . In this case, a strain of 1.0% was applied to conduct the measurements within the linear viscoelastic region, which was determined by dynamic strain sweep experiment. For the investigation of hydrogel



strength and relaxation exponent, stress relaxation analyses were conducted at 25 °C. In this case, each hydrogel sample was subjected to a rapid applied small strain, which was held constant for the remainder of the experiment, and the decay of stress in the viscoelastic material was monitored as a function of time. In this case, the hydrogel sample was allowed to consolidate for 12 h before beginning the analysis. The strain applied to the hydrogel sample increased from 0.1 to 100% (1 rad s<sup>-1</sup> and 25 °C).

### Determination of the minimum inhibition concentration (MIC)

*Staphylococcus aureus* (*S. aureus*, Gram-positive bacteria) and *Escherichia coli* (*E. coli*, Gram-negative bacteria) were used for antibacterial tests.<sup>33</sup> At first, a single colony of *S. aureus* and *E. coli* on the solid LB agar plate was transferred into 5 mL of liquid LB culture medium grown at 37 °C for 24 h. The bacterial suspension was then diluted with LB culture medium to  $1 \times 10^5$  CFU mL<sup>-1</sup>. Different kinds of polymers at predetermined concentrations (from 2 µg mL<sup>-1</sup> to 500 µg mL<sup>-1</sup>) were mixed with an equal volume of the diluted bacterial suspension and incubated at 37 °C for 24 h. Finally, the OD<sub>600</sub> value of the solution was determined by a microplate reader Varioscan Flash. Samples treated with deionized water were used as controls, and each assay was repeated three times.

### Sustained release of silver ions

The release of silver ions from the coordination polymers was performed in phosphate buffer (10 mM, pH 7.4).<sup>9</sup> Briefly, 1 mL of the Ag(I)-load polymer solution (at a final Ag<sup>+</sup> concentration of 1.0 mg mL<sup>-1</sup>) was introduced into a dialysis bag (Spectra/Pore, MWCO = 1000 Da) and then immersed in 25 mL of buffer solution at 37 °C. At certain time intervals, 1 mL of the dialysis solution was taken out to measure the silver concentration, and another 1 mL of fresh buffer solution was added. The cumulative release of silver ions was determined by ICP-MS, and the release experiments were conducted in triplicate.

### Biofilm preparation

Amoxicillin-resistant *E. coli* and methicillin-resistant *S. aureus* biofilms were prepared in 96-well plates. Briefly, amoxicillin-resistant *E. coli* and methicillin-resistant *S. aureus* cells were suspended in a TSB medium with the initial density of  $1 \times 10^6$  cells per mL. Approximately 100 µL suspensions were transferred into 96-well plates and incubated at 37 °C for 24 h. The supernatants were discarded, and non-adherent cells were removed by washing the biofilms three times with sterile PBS. The preformed biofilms were directly exposed to the polymer hydrogel **Ag/1c** and AgNO<sub>3</sub>.

### Contact-mediated killing kinetics of the polymer hydrogel **Ag/1c**

Amoxicillin-resistant *E. coli* and methicillin-resistant *S. aureus* preformed biofilms were incubated with 100 µL-aliquots of TSB medium with various concentrations of the polymer hydrogel

**Ag/1c**. After 1 h of incubation, samples were withdrawn in 10 mL PBS, centrifuged, then serially diluted in PBS and plated on LB agar plates for survival colony counting.

### Cytotoxicity assay

*In vitro* cytotoxicity was assessed by the MTT assay.<sup>34</sup> Briefly, human embryonic kidney cells (293T cells, 5000/well) were seeded in 96-well culture plates and incubated at 37 °C/5% CO<sub>2</sub>. After 24 h, culture media was removed, and fresh media (200 µL) containing the free compounds **1a–c**, AgNO<sub>3</sub>, and **Ag/1c** at various Ag<sup>+</sup> concentrations ranging from 1.39 µg mL<sup>-1</sup> to 250 µg mL<sup>-1</sup> were added to each well. Cells without any treatment were set as control. After 24 h, the culture media was removed, fresh media (100 µL) containing MTT (5 µL) was added to each well, and the plates were incubated at 37 °C for another 2 h. Formazan crystals were dissolved in dimethyl sulfoxide (DMSO) after 2 h. The absorbance of the entire solution was evaluated at 490 nm for each sample, measured using a microplate reader Varioscan Flash.

## Results and discussion

### Synthesis and characterization of the antibacterial coordination polymer hydrogels **Ag/1a–c**

The water-soluble ligands **1a–c** were simply prepared by Ullmann cross-coupling between commercially available 3,5-dibromobenzyl alcohol and imidazole and alkylation of the resulting 3,5-diimidazolylbenzyl alcohol with sulfonated poly(ethylene glycol)s (PEGs) in the presence of sodium hydroxide (see the ESI for details†). The PEGs were employed as the hydrophilic segments due to their commercial availability and FDA-approved biocompatibility,<sup>35,36</sup> and three different PEGs were designed to investigate the effect of chain lengths on the antibacterial activity. Generally, the coordination polymer hydrogels **Ag/1a–c** are formed by adding an aqueous solution of **1a–c** to an aqueous solution of AgNO<sub>3</sub> under shaking at room temperature in the absence of light (See Experimental for details). To our surprise, although the critical gel concentration (CGC) of Ag(I)-1,3-bisimidazolyl benzene could be as low as 0.3 wt% at a 1 : 1 ratio of AgNO<sub>3</sub> : ligand,<sup>32</sup> when 1 : 1 ratio of AgNO<sub>3</sub> : ligands **1a–c** was employed, even with the concentration of up to 5 wt%, no gelation occurred in water. We rationalized that the weak coordination of the PEG chains with Ag(I) might consume partial silver ions;<sup>37–39</sup> this reduced the amount of silver ions used for coordination with *N* to form coordination polymers and thus hindered the formation of the hydrogels. As expected, when more silver ions were added, transparent gelation was achieved under the CGCs less than 2 wt% (Table 1). Different PEG chains require different AgNO<sub>3</sub> : ligand ratios; the longer the PEG chains, the higher the silver ion : ligand ratios.

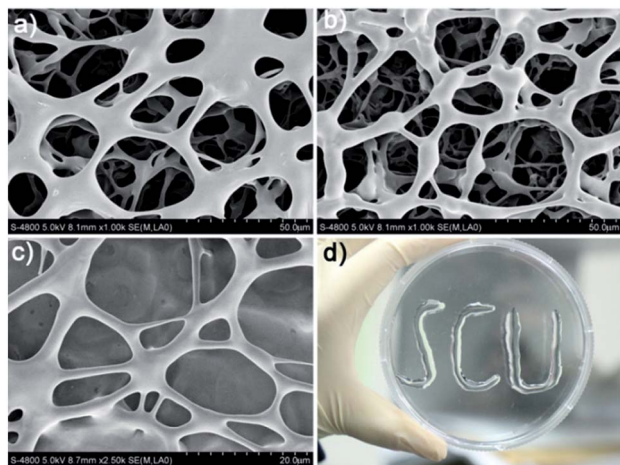
The scanning electron microscopy (SEM) measurement clearly revealed the supramolecular structure of the coordination polymer hydrogels. As shown in Fig. 1, the SEM images obtained for the freeze-dried hydrogel (xerogel) demonstrated the formation of well-developed three-dimensional networks





**Table 1** Minimum ratio and CGCs of the Ag(I)-ligands **1a–c** used for the fabrication of hydrogels

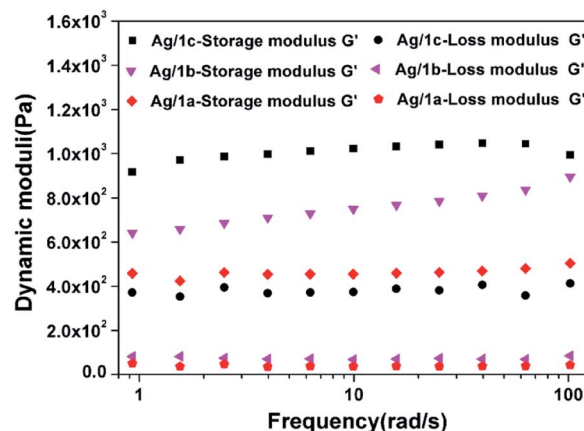
Entry	Ligand	Ag(I) : ligand (mol mol <sup>-1</sup> )	CGC (wt%)
1	<b>1a</b>	1.5 : 1	1.4
2	<b>1b</b>	2.5 : 1	1.8
3	<b>1c</b>	3.0 : 1	2.0

**Fig. 1** SEM images of the coordination polymer hydrogels formed by AgNO<sub>3</sub> with (a) **1a**, (b) **1b**, and (c) **1c**. (d) An image of the characters "SCU" injected by the coordination polymer hydrogel formed by **Ag/1c** with a 3 mL glass syringe.

composed of interlocked fibers with length up to several micrometers that would be responsible for gelation. Notably, the ribbon-like bundles with diameter in the order of micrometers are observed in the field of view, which should be aggregated by nano-fibers during the drying process. To further characterize the nano-fibers, transmission electron microscopy (TEM) was conducted. As shown in Fig. 1S,<sup>†</sup> the TEM image obtained for the gel of **Ag/1c** indeed shows the presence of well-grown distinct fibrillar assemblies with a diameter of ~10 nm. It should be mentioned that these formed hydrogels have excellent stability and can remain stable over a period of several months at ambient temperature with negligible change. More interestingly, the formed hydrogels possess outstanding ductility and could form an arbitrary shape by simple injection with an ordinary syringe (Fig. 1d); this indicates great potential for the practical applications of the coordination polymer hydrogels, especially for application in surface antibiosis of various equipment.

### Mechanical strength of the coordination polymer hydrogels

Fig. 2 shows the frequency sweep profiles of storage modulus ( $G'$ ) and loss modulus ( $G''$ ) at 25 °C for the coordination polymers **Ag/1a–c**. We can find that for all three samples, the  $G'$  values are greater than the  $G''$  values over the entire frequency range; this suggests that the hydrogels are formed. Notably, compared to the hydrogels formed by **Ag/1a** and **Ag/1b**, the

**Fig. 2** Storage modulus ( $G'$ ) and loss modulus ( $G''$ ) as a function of angular frequency for the coordination polymer hydrogels formed by **Ag/1a**, **Ag/1b**, and **Ag/1c**.

hydrogel of **Ag/1c** demonstrated obvious improvement of  $G'$  and  $G''$ . Taking the frequency of 20.0 rad s<sup>-1</sup> as example, the  $G'$  and  $G''$  values of **Ag/1c** were measured to be 1032.5 Pa and 389.3 Pa, whereas they were only 767.9 Pa and 70.7 Pa for the **Ag/1b** hydrogel and 459.3 Pa and 38.0 Pa for the **Ag/1a** hydrogel, respectively. This result indicates that the **Ag/1c** hydrogel holds a higher mechanical strength than the **Ag/1a** and **Ag/1b** hydrogels.

### Antimicrobial activity of the coordination polymer hydrogels

The antimicrobial properties of the three coordination polymer hydrogels were determined by the minimum inhibitory concentration (MIC), a standard microbiological technique used to evaluate the bacteriostatic activity of antimicrobial agents. Silver nitrate was used as the reference standard, and the Gram-positive (*Staphylococcus aureus*, *S. aureus*) and Gram-negative (*Escherichia coli*, *E. coli*) pathogens of common clinical interest were employed as test organisms. Upon mixing the coordination polymer at predetermined concentration with the bacterial suspension in the LB broth culture medium and incubating at 37 °C for 24 h, the OD<sub>600</sub> value of the solution was obtained by a spectrophotometer (see Experimental section for details). The MIC was obtained by visual inspection of the turbidity of the solution, and the results are listed in Table 2. As expected, all three kinds of coordination polymers show much

**Table 2** Minimum inhibitory concentrations (MICs) of antibacterial coordination polymer hydrogels and silver nitrate for *E. coli* and *S. aureus*

Entry	Coordination polymer	MIC (μg mL <sup>-1</sup> )	
		<i>S. aureus</i>	<i>E. coli</i>
1	<b>Ag/1a</b>	6.95	4.95
2	<b>Ag/1b</b>	4.29	3.29
3	<b>Ag/1c</b>	2.14	2.44
4	AgNO <sub>3</sub>	32.5	10.62



higher antimicrobial activity than silver nitrate for both *E. coli* and *S. aureus*. Especially for the coordination polymer **Ag/1c**, the MICs could be as low as  $2.14 \mu\text{g mL}^{-1}$  for *S. aureus* and  $2.44 \mu\text{g mL}^{-1}$  for *E. coli*, which were up to 15.2 times and 4.4 times lower than that of silver nitrate, respectively. It should be noted that the ligands themselves have no activity (Fig. 2S†); this indicates that the high antimicrobial activity originates from Ag(I) attached on the coordination polymer fibers instead of the ligands. Interestingly, we can find that the coordination polymer hydrogels with longer PEG chains possess more effective antibacterial activity. This can be attributed to the long chain PEGs that provide the formed coordination polymer with higher surface area to contact bacteria and thus achieve a better antibacterial effect.

### Sustained release of silver(I) from the antibacterial coordination polymer hydrogels

As abovementioned, the long-term sustained release of silver ions from the matrix is very important for biomedical applications. We then tested the release behavior of silver ions from the coordination polymers by equilibrium dialysis at  $37^\circ\text{C}$  in 10.0 mM PBS buffer at pH 7.4. At predetermined periods, 1.0 mL of the solution was obtained from the reservoirs, and the samples were analyzed by ICP-MS. As plotted in Fig. 3, it is clearly shown that all three samples exhibit sustained release feature, and the release ratios of Ag(I) at the time point of 120 h are 14.5%, 30.5%, and 51.2% for **Ag/1a**, **Ag/1b**, and **Ag/1c**, respectively. It was found that **Ag/1c** demonstrated a faster release rate than the other two samples. This is reasonable since Ag ions protected in the coordination polymer **Ag/1c** are more coordinated with the ether bonds of PEG chains, whose coordination ability is not as strong as that of the imidazolyl moieties.<sup>40</sup> Thus, the faster release behavior might be partially responsible for the higher antibacterial activity.

### Antimicrobial activity of the coordination polymer hydrogels against drug-resistant bacteria

Encouraged by the excellent performance of the silver-containing coordination polymer hydrogels against common

**Table 3** Minimum inhibitory concentrations (MICs) of antibacterial coordination polymer hydrogels and silver nitrate for MDR *S. aureus* and *E. coli*

Entry	Coordination polymer	MIC ( $\mu\text{g mL}^{-1}$ )	
		MRSA	AREC
1	<b>Ag/1a</b>	37.5	42.5
2	<b>Ag/1b</b>	31.3	37.5
3	<b>Ag/1c</b>	15.6	15.6
4	$\text{AgNO}_3$	75.0	62.5

bacteria, we further tested their antimicrobial activity over the multidrug-resistant (MDR) bacteria. To the best of our knowledge, there are no reports on the use of silver-loaded nanofibers against MDR bacteria. Herein, the MDR organisms methicillin-resistant *S. aureus* (MRSA) and amoxicillin-resistant *E. coli* (AREC) were used for the antibacterial tests, and the activity of the coordination polymers was also determined by MIC measurement. To our delight, all three coordination polymer hydrogels showed good antibacterial performance similar to that against common bacteria (Table 3). It should be particularly noted that the antibacterial coordination polymer hydrogel seems to possess special activity to kill methicillin-resistant *S. aureus*. Even for the coordination polymer **Ag/1a** with short PEG chains, its antimicrobial efficiency could provide a comparable kill rate to that of  $\text{AgNO}_3$  against common *S. aureus*. The coordination polymer **Ag/1c** with longer PEG chains performed much better, and its MIC could be as low as  $15.6 \mu\text{g mL}^{-1}$ ,  $\sim 4.8$  times lower than that of silver nitrate ( $75.0 \mu\text{g mL}^{-1}$ ).

### Contact-killing kinetics of the coordination polymer hydrogels over drug-resistant bacteria

The formation of biofilms, which have been associated with a variety of multi-resistant bacterial strains and resilient infections, is the main reason of microbial infections.<sup>41</sup> To further demonstrate the application superiority of the coordination polymer hydrogels, the contact-killing test over methicillin-resistant *S. aureus* and amoxicillin-resistant *E. coli* taking **Ag/1c** as an example has been investigated. After culturing the biofilms with the hydrogel **Ag/1c** for 1 h, we found that both the amoxicillin-resistant *E. coli* and methicillin-resistant *S. aureus* cells exposed to the coordination polymer hydrogel **Ag/1c** were sharply killed at  $35 \mu\text{g mL}^{-1}$ ; however,  $50 \mu\text{g mL}^{-1}$   $\text{AgNO}_3$  could only have caused about 50% growth reduction for amoxicillin-resistant *E. coli* and methicillin-resistant *S. aureus* cells (Fig. 4). This suggests that surface contact of the coordination polymer hydrogels is a promising approach of eradicating MDR bacteria to prevent the formation of the biofilms.

### Cytotoxicity assay

As is known, biocompatibility is of great importance for an antibacterial material in human-related applications. The cytotoxicity of coordination polymer hydrogels to mammalian cells was then investigated by evaluating cell viability using the MTT assay after 24 h culture in Human embryonic kidney 293T

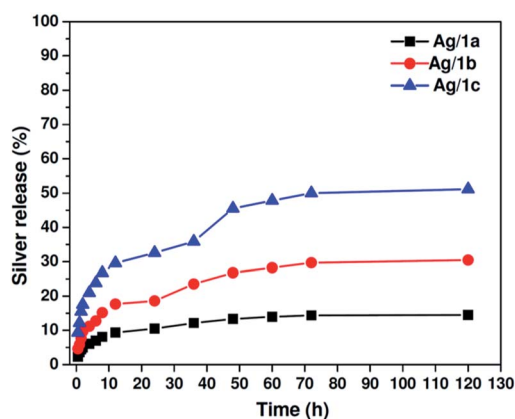


**Fig. 3** Cumulative release profiles of silver from the coordination polymers **Ag/1a–c** at  $37^\circ\text{C}$  in 10.0 mM PBS at pH 7.4.



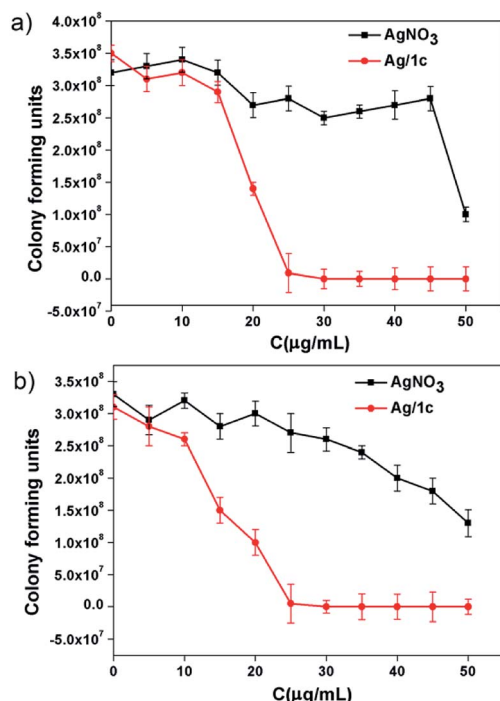


Fig. 4 The contact-killing effect of the polymer hydrogel **Ag/1c** on (a) amoxicillin-resistant *E. coli* biofilms; (b) methicillin-resistant *S. aureus* biofilms were treated with different concentrations and incubated at 37 °C for 1 h. The corresponding concentrations of silver nitrate were used as the control group. The survival rates were then calculated based on the survival colonies. The results are shown as the averages with standard deviations (error bars) from three independent experiments.

cells with different concentrations of **Ag/1c** and  $\text{AgNO}_3$ . As shown in Fig. 5, the results of the cytotoxicity study indicate that **Ag/1c** is significantly less cytotoxic than  $\text{AgNO}_3$ . At a silver ion concentration of 25  $\mu\text{g mL}^{-1}$ , the cells treated with **Ag/1c** showed up to 100% viability, whereas the survival rate for

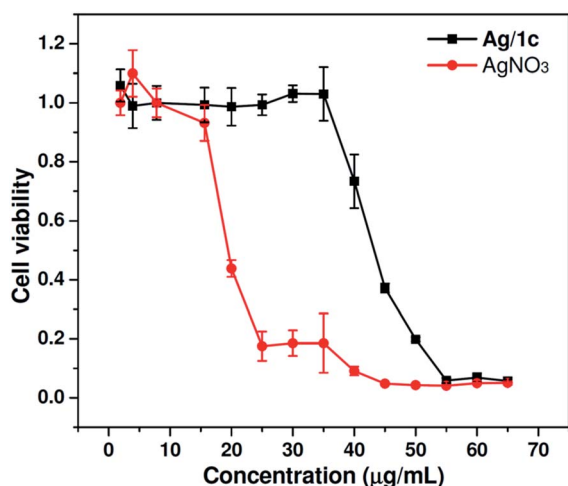


Fig. 5 *In vitro* cytotoxicity of **Ag/1c** and  $\text{AgNO}_3$  against 293T cells after incubation for 24 h at 37 °C with a series of concentrations. 293T cells incubated without any materials were used as the control (mean  $\pm$  SD,  $n = 6$ ).

$\text{AgNO}_3$ -treated cells was only 17%. Even at a high concentration of 40  $\mu\text{g mL}^{-1}$ , the viabilities of the **Ag/1c**-treated cell can still remain nearly  $\sim 80\%$ . The  $\text{IC}_{50}$  for **Ag/1c** was calculated to be 42.5  $\mu\text{g mL}^{-1}$ , which was around 2.5 times lower than that of  $\text{AgNO}_3$  (17.0  $\mu\text{g mL}^{-1}$ ). The control experiment discloses that the compound **1a-c** showed negligible cytotoxicity up to a concentration of 250.0  $\mu\text{g mL}^{-1}$  in 293T cells (Fig. 3S†). The abovementioned results thus demonstrate that **Ag/1** reduces the cytotoxicity of silver ions and possesses great potential for clinical use because of its good cytocompatibility and enhanced antibacterial activity.

## Conclusions

In conclusion, the coordination polymer hydrogels, consisting of silver(I)-PEGylated bisimidazolylbenzyl alcohol, were used for the first time as an antibacterial agent, which showed much higher antibacterial activity than silver nitrate for both Gram-positive and Gram-negative bacteria. Even against the drug-resistant bacteria, they showed better bactericidal performance. The experimental results suggested that the high antibacterial activity resulted from the synergistic effect of improved stability of silver ions, increased contact area with bacteria, and sustained release of silver ions from the coordination polymer matrix. Notably, upon improving the antibacterial effect, the cytotoxicity of silver ions to mammalian cells was reduced remarkably. In short, easier preparation method, improved stability, outstanding ductility, sustained releasability, low cytotoxicity, and most importantly, high antibacterial activity would make the antibacterial coordination polymer hydrogels highly attractive for various applications such as in clinical burn and wound dressing, biofilms, bioadhesives, and coatings of biomedical materials.

## Conflicts of interest

The authors have no conflicts of interest to declare for this article.

## Acknowledgements

This work was supported by the National Natural Science Foundation of China (No. 51673130, 21372170), the Excellent Young Foundation of Sichuan Province (2014JQ0032 and 2016JQ0028), and the Applied Basic Research Project of Sichuan Province (15JC0440).

## Notes and references

- G. A. Sotiriou, A. Meyer, J. T. N. Knijnenburg, J. T. Panke and S. E. Pratsinis, *Langmuir*, 2012, **28**, 15929–15936.
- K. Jamuna-Thevi, S. A. Bakar, S. Ibrahim, N. Shahab and M. R. M. Toff, *Vacuum*, 2011, **86**, 235–241.
- R. Kumar and H. Münstedt, *Biomaterials*, 2005, **26**, 2081–2088.
- K. Ziegler, R. Görl, J. Effing and J. Ellermann, *Skin Pharmacol. Physiol.*, 2006, **19**, 140–146.



- 5 B. LeOuay and F. Stellacci, *Nano Today*, 2015, **10**, 339–354.
- 6 X. Zeng, D. T. McCarthy and A. Deletic, *Adv. Funct. Mater.*, 2015, **25**, 4344–4351.
- 7 Y. Lin, K. Xiong and Z. Lu, *Chem. Commun.*, 2017, **53**, 9777–9780.
- 8 L. Mei, Z. Teng, G. Zhu, Y. Liu, F. Zhang, J. Zhang and Q. Wang, *ACS Appl. Mater. Interfaces*, 2017, **9**, 35297–35304.
- 9 F. Huang, Y. Gao and Y. Zhang, *ACS Appl. Mater. Interfaces*, 2017, **9**, 16880–16889.
- 10 X. Wang, S. Zhu, L. Liu and L. Li, *ACS Appl. Mater. Interfaces*, 2017, **9**, 9051–9058.
- 11 A. GhavamiNejad, A. R. Unnithan, A. R. Sasikala, M. S. Samarihalaj, R. G. Thomas, Y. Y. Jeong, S. Nasser, P. Murugesan, D. M. Wu and C. S. Kim, *ACS Appl. Mater. Interfaces*, 2015, **7**, 12176–12183.
- 12 C. Marambio-Jones and E. M. Hoek, *J. Nanopart. Res.*, 2010, **12**, 1531–1551.
- 13 C. Fasting, C. A. Schalley, M. Weber, O. Seitz, S. Hecht and B. Koks, *Angew. Chem., Int. Ed.*, 2012, **51**, 10472–10498.
- 14 S. Bhatia, C. L. Cuellar and R. Haag, *J. Am. Chem. Soc.*, 2016, **138**, 8654–8666.
- 15 K. A. Rieger, H. J. Cho and H. F. Yeung, *ACS Appl. Mater. Interfaces*, 2016, **8**, 3032–3040.
- 16 P. O. Rujitanaroj, N. Pimpha and P. Supaphol, *Polymer*, 2008, **49**, 4723–4732.
- 17 A. Melaiye, Z. Sun, K. Hindi, A. Milsted, D. Ely and W. J. Youngs, *J. Am. Chem. Soc.*, 2005, **127**, 2285–2291.
- 18 F. Zheng, S. Wang, S. Wen, M. Shen, M. Zhu and X. Shi, *Biomaterials*, 2013, **34**, 1402–1412.
- 19 A. R. Unnithan, N. A. M. Barakat and P. B. T. Pichiah, *Carbohydr. Polym.*, 2012, **90**, 1786–1793.
- 20 J. H. Park, M. R. Karim, I. K. Kim, I. W. Cheong, J. W. Kim and D. G. Bae, *Colloid Polym. Sci.*, 2010, **288**, 115–121.
- 21 J. M. Lehn, *Supramolecular Chemistry Concepts and Perspectives*, VCH, Weinheim, 1995.
- 22 G. Férey, C. Mellot-Draznieks, C. Serre and F. Millange, *Acc. Chem. Res.*, 2005, **38**, 217–225.
- 23 J. T. Hupp and K. R. Poeppelmeier, *Science*, 2005, **309**, 2008–2009.
- 24 S. Kitagawa, R. Kitaura and S. Noro, *Angew. Chem., Int. Ed.*, 2004, **43**, 2334–2375.
- 25 A. T. M. Fiori, D. H. Nakahata, A. Cuin, W. R. Lustri and P. P. Corbi, *Polyhedron*, 2017, **121**, 172–179.
- 26 S. W. Jaros, G. D. S. Mf, J. Król, O. M. Conceição, p. Smoleński and A. Pombeiro, *Inorg. Chem.*, 2016, **55**, 1486–1496.
- 27 M. Berchel, T. L. Gall, C. Denis, S. L. Hir, F. Quentel and C. Elleouet, *New J. Chem.*, 2011, **35**, 1000–1003.
- 28 S. Patil, A. Deally, B. Gleeson, H. Müllerbunz, F. Paradisi and M. Tacke, *Metallomics*, 2011, **3**, 74–88.
- 29 A. Kascatannebioglu, A. Melaiye, K. Hindi, S. Durmus, M. J. Panzner and L. A. Hogue, *J. Med. Chem.*, 2006, **49**, 6811–6818.
- 30 K. M. Hindi, T. J. Siciliano, S. Durmus, M. J. Panzner, D. A. Medvetz and D. V. Reddy, *J. Med. Chem.*, 2008, **51**, 1577–1583.
- 31 A. Melaiye, R. S. Simons, A. Milsted, F. Pingitore, C. Wesdemiotis, C. A. Tessier and W. J. Youngs, *J. Med. Chem.*, 2004, **47**, 973–977.
- 32 S. Zhang, S. Yang, J. Lan, S. Yang and J. You, *Chem. Commun.*, 2008, 6170–6172.
- 33 J. M. Andrews, *J. Antimicrob. Chemother.*, 2001, **48**, 5.
- 34 C. Liao, Y. Chen, Y. Yao, S. Zhang, Z. Gu and X. Yu, *Chem. Mater.*, 2016, **28**, 7757–7764.
- 35 S. Zhang, W. Yao, W. He, K. Luo and Z. Gu, *Sci. China: Chem.*, 2014, **57**, 461–475.
- 36 K. Knop, R. Hoogenboom, D. Fischer and U. S. Schubert, *Angew. Chem., Int. Ed.*, 2010, **49**, 6288–6308.
- 37 N. Fleitas-Salazar, E. Silva-Campa and S. J. Pedrosa-Santana, *J. Nanopart. Res.*, 2017, **19**, 113.
- 38 Z. Sun, F. Lv and L. Cao, *Angew. Chem., Int. Ed.*, 2015, **54**, 7944–7948.
- 39 S. Zhang, G. Qiu and Y. P. Ting, *Colloids Surf., A*, 2013, **436**, 207–214.
- 40 A. Thalera, R. Bergtera, T. Ossowskib, B. G. Cox and H. Schneider, *Inorg. Chim. Acta*, 1999, **285**, 1–9.
- 41 D. Lebeaux, J. M. Ghigo and C. Beloin, *Microbiol. Mol. Biol. Rev.*, 2014, **78**, 510–543.

